

OPTIMUM UNDULATOR TAPERING OF SASE FEL: FROM THE THEORY TO EXPERIMENT

E.A. Schneidmiller, M.V. Yurkov, DESY, Hamburg, Germany

Abstract

In this report we present recent results of the experimental studies at FLASH2 free electron laser on application of undulator tapering for efficiency increase. Optimization of the amplification process in FEL amplifier with diffraction effects taken into account results in a specific law of the undulator tapering [1–3]. It is a smooth function with quadratic behavior in the beginning of the tapering section which transforms to a linear behavior for a long undulator. Obtained experimental results are in reasonable agreement with theoretical predictions.

UNIVERSAL TAPERING LAW

Effective energy exchange between the electron beam moving in an undulator and electromagnetic wave happens when resonance condition takes place. When amplification process enters nonlinear stage, the energy losses by electrons become to be pronouncing which leads to the violation of the resonance condition and to the saturation of the amplification process. Application of the undulator tapering [4] allows to a further increase of the conversion efficiency. An idea is to adjust undulator parameters (field or period) according to the electron energy loss such that the resonance condition is preserved. Undulator tapering has been successfully demonstrated at long wavelength FEL amplifiers [5, 6], and is routinely used at x-ray FEL facilities LCLS and SACLA [7, 8]. In the framework of the one-dimensional theory an optimum law of the undulator tapering is quadratic [9–15]. Similar physical situation occurs in the FEL amplifier with a waveguide [5]. Parameters of FEL amplifiers operating in the infrared, visible, and x-ray wavelength ranges are such that diffraction of radiation is an essential physical effect influencing optimization of the tapering process. In the limit of thin electron beam (small value of the diffraction parameter) linear undulator tapering works well from almost the very beginning [12]. It has been shown in [10] that: i) tapering law should be linear for the case of thin electron beam, ii) optimum tapering at the initial stage should follow quadratic dependence, iii) tapering should start approximately two field gain length before saturation.

Comprehensive analysis of the problem of the undulator tapering in the presence of diffraction effects has been performed in [1–3]. It has been shown that the key element for understanding the physics of the undulator tapering is given by the model of the modulated electron beam which provides relevant interdependence of the problem parameters. Finally, application of similarity techniques to the results of numerical simulations led to the universal law of the undulator tapering:

$$\hat{C} = \alpha_{tap}(\hat{z} - \hat{z}_0) \left[\arctan\left(\frac{1}{2N}\right) + N \ln\left(\frac{4N^2}{4N^2 + 1}\right) \right], \quad (1)$$

with Fresnel number N fitted by $N = \beta_{tap}/(\hat{z} - \hat{z}_0)$. Undulator tapering starts by two field gain length $2 \times L_g$ before the saturation point at $z_0 = z_{sat} - 2 \times L_g$. Parameter β_{tap} is rather well approximated with the linear dependency on diffraction parameter, $\beta_{tap} = 8.5 \times B$. Parameter α_{tap} is a slow varying function of the diffraction parameter B , and scales approximately to $B^{1/3}$. Analysis of the expression (1) shows that it has quadratic dependence in z for small values of z (limit of the wide electron beam), and linear dependence in z for large values of z (limit of the thin electron beam).

ANALYSIS OF TAPERING PROCESS

Seeded FEL

Red curve in Fig. 1 shows evolution of the average radiation power of seeded FEL along the optimized tapered undulator. Significant amount of particles is trapped in the regime of coherent deceleration (top plot in Fig. 2). The particles in the core of the beam are trapped most effectively. Nearly all particles located at the edge of the electron beam leave the stability region very soon. The trapping process lasts for a several field gain lengths when the trapped particles become to be isolated in the trapped energy band for which the undulator tapering is optimized further. For large values of the diffraction parameter $B \gtrsim 10$ the trapping process is not finished even at three field gain lengths after saturation, and non-trapped particles continue to populate low energy tail of the energy distribution (see Fig. 3). There was an interesting experimental observation at LCLS that energy distribution of non-trapped particles is not uniform, but represent a kind of energy bands [17, 18]. Graphs presented in Fig. 2 give a hint on the origin of energy bands which are formed by non-trapped particles. This is the consequence of nonlinear dynamics of electrons leaving the region of stability.

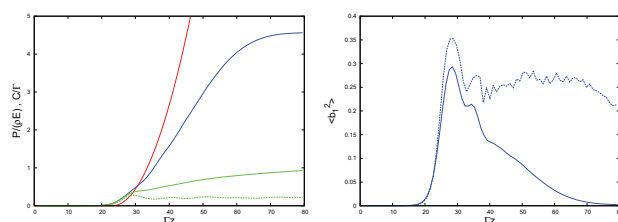


Figure 1: Left: Evolution along the undulator of the reduced radiation power $\hat{\eta} = W/(\rho W_{beam})$. Red and blue lines correspond to the case of tapered seeded and SASE FEL. Green dashed and solid lines refer the case of untapered seeded and SASE FEL. Right: Evolution along the undulator of the squared value of the bunching factor for the FEL amplifier with optimized undulator tapering. Dashed and solid line represent seeded and SASE FEL, respectively. Diffraction parameter is $B = 10$. Simulations are performed with code FAST [16].

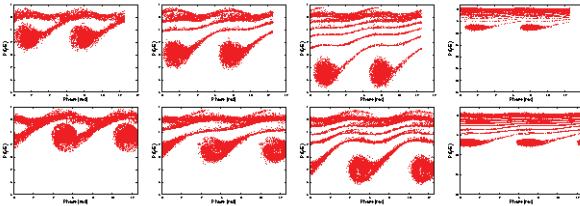


Figure 2: Phase space distribution of electrons in the tapering regime. Diffraction parameter is $B = 10$. Plots from the left to the right correspond to $\hat{z} = 36, 40, 44$ and 50 , respectively. Upper row represents seeded FEL amplifier. Lower row represents SASE FEL at the coordinate along the bunch $\hat{s} = \rho\omega t = 100$, see Fig. 4. Simulations are performed with code FAST [16].

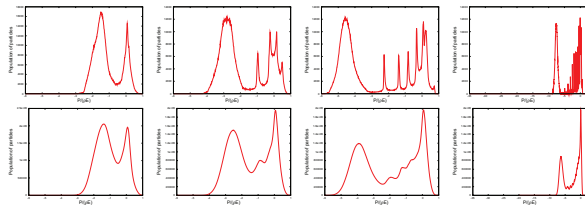


Figure 3: Population of the particles in energy at different stages of amplification. Diffraction parameter is $B = 10$. Plots from the left to the right correspond to $\hat{z} = 36, 40, 44$ and 50 , respectively. Upper and lower rows represent seeded FEL amplifier and SASE FEL, respectively. Simulations are performed with code FAST [16].

Note that a similar effect can be seen in the early one-dimensional studies [13, 14].

SASE FEL

The considerations on the strategy for the tapering optimization of a SASE FEL is rather straightforward. Radiation of SASE FEL consists of wavepackets (spikes). In the exponential regime of amplifications wavepackets interact strongly with the electron beam, and their group velocity visibly differs from the velocity of light. In this case the slippage of the radiation with respect to the electron beam is by several times less than kinematic slippage [15]. This feature is illustrated with the upper plot in Fig. 4 which shows onset of the nonlinear regime. We see that wavepackets are closely connected with the modulations of the electron beam current. When the amplification process enters nonlinear (tapering) stage, the group velocity of the wavepackets approaches to the velocity of light, and the relative slippage approaches to the kinematic one. When a wavepacket advances such that it reaches the next area of the beam disturbed by another wavepacket, we can easily predict that the trapping process will be destroyed, since the phases of the beam bunching and of the electromagnetic wave are uncorrelated in this case. Typical scale for the destruction of the tapering regime is coherence length, and the only physical mechanism we can use is to decrease the group velocity of wavepackets. This happens optimally when we trap maximum of the particles in the regime of coherent deceleration, and force these particles to interact as strong as possible with the electron beam. We see that this strategy is exactly the same as we used for optimization of seeded FEL. Global numerical optimization confirms these simple physical considerations. Conditions of the optimum tapering are the same as it has been described above for the seeded case. Start of the tapering is by two field gain lengths before the saturation. Parameter β_{tap}

ISBN 978-3-95450-182-3

2640

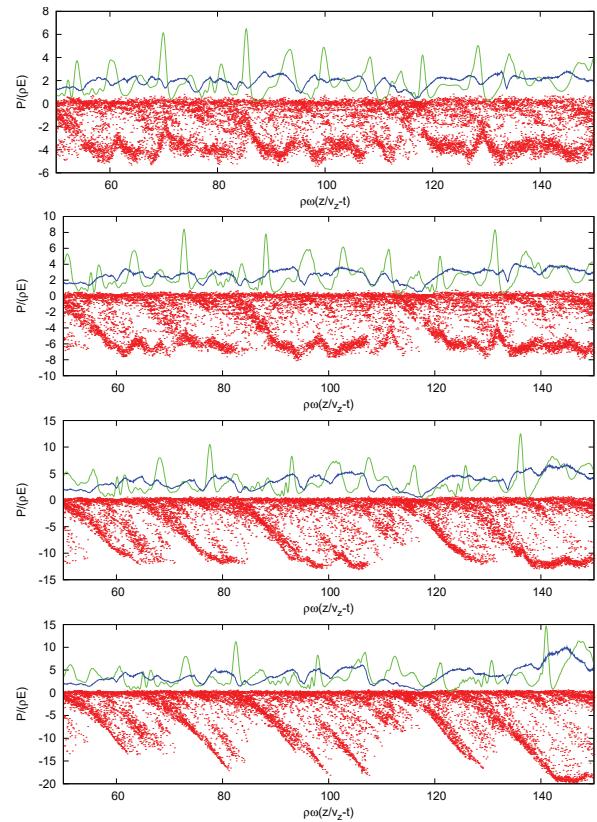


Figure 4: Phase space distribution of the particles along the bunch (red dots), average loss of the electron energy (blue line), and radiation power (green line) in the deep tapering regime. Diffraction parameter is $B = 10$. Plots from the top to the bottom correspond to $\hat{z} = 44, 50, 60$, and 70 , respectively. Simulations are performed with code FAST [16].

is the same, $8.5 \times B$. The only difference is the reduction of the parameter α_{tap} by 20% which is natural if one remember statistical nature of the wavepackets. As a result, optimum detuning is just 20% below the optimum seeded case.

Figure 1 shows evolution of the average radiation power of SASE FEL along optimized tapered undulator. Details of the phase space distributions are traced with Figs. 2 and 4. Initially behavior of the process is pretty close to that of the seeded case. Initial values of the beam bunching is comparable with the seeded case (see Fig. 1). The rate of the energy growth is also comparable with the seeded case. The feature of the "energy bands" remains clearly visible in the case of SASE FEL as well (see Fig. 3). It is interesting observation that plots in Figs. 4 corresponding to the well trapped particles qualitatively correspond to experimental data from LCLS taken with transverse deflecting cavity [17, 18].

The beam bunching gradually drop down when wavepackets travel along the bunch. As we expected, the amplification process is almost abruptly stopped when the relative slippage exceeded the coherence length. However, increase of the total radiation power with respect to the saturation power is about factor of 10.

EXPERIMENTAL RESULTS

Free electron laser FLASH is equipped with two undulator beam-lines [19–21]. Fixed gap undulator (period 2.73 cm, peak magnetic field 0.48 T, total magnetic length 27 m) is installed in the first

02 Photon Sources and Electron Accelerators

A06 Free Electron Lasers

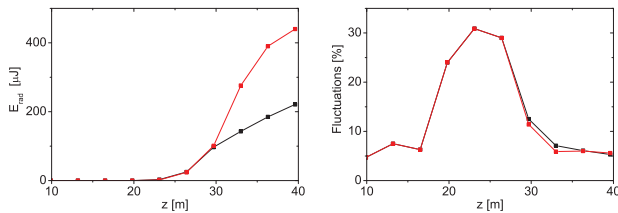


Figure 5: Pulse energy (left plot) and fluctuations of the radiation pulse energy (right plot) versus undulator length measured at FLASH2. Electron energy is 680 MeV, radiation wavelength is 32 nm, bunch charge is 300 pC. Color codes are: red for untapered case and black for optimum undulator tapering.

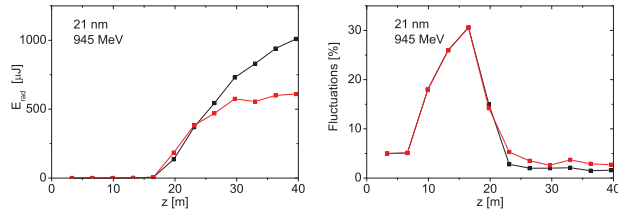


Figure 6: Pulse energy (left plot) and fluctuations of the radiation pulse energy (right plot) versus undulator length measured at FLASH2. Electron energy is 945 MeV, radiation wavelength is 21 nm, bunch charge is 400 pC. Color codes are: red for untapered case and black for optimum undulator tapering.

beamline, FLASH1. The second beam line, FLASH2, is equipped with variable gap undulator (period 3.14 cm, maximum peak magnetic field 0.96 T, total magnetic length 30 m). With operating range of the electron beam energies of 0.4 - 1.25 GeV FLASH1 and FLASH 2 beamline cover wavelength range from 4-52 nm and 3.5-90 nm, respectively.

Experiment on undulator tapering has been performed at FLASH2. Undulator consists of 12 modules of 2.5 meter length separated with intersections. Two modes of undulator tapering can be implemented: step tapering and smooth tapering. Procedure of the step tapering applies step change of the undulator gap from module to module, and smooth tapering assumes additional linear change of the gap along each module. During experiment only step tapering mode was available. Experimental procedure for tuning of the tapering parameters involves statistical measurements of the radiation energy. Optimum conditions of the undulator tapering assume the starting point to be by two field gain lengths before the saturation point corresponding to the maximum brilliance of the SASE FEL radiation [22]. Saturation point on the gain curve is defined by the condition for fluctuations to fall down by a factor of 3 with respect to their maximum value in the end of exponential regime. Then quadratic law of tapering is applied (optimal for moderate increase of the extraction efficiency at the initial stage of tapering. This experimental techniques has been successfully tested at FLASH2 as illustrated in Figs. 5 and 6. For the case shown in Fig. 6 saturation occurs at the undulator length of 20 meters, and saturation energy is about 150 μ J. Optimized tapering increases the pulse energy by a factor of 6, up to 1000 μ J. Untapered undulator

delivers only 610 μ J at full undulator length of 40 meters. Thus, tapering of the FLASH2 undulator demonstrates great benefit in the increase of the radiation pulse energy.

REFERENCES

- [1] E.A. Schneidmiller and M.V. Yurkov, Proc. FEL2014 Conference, Basel, Switzerland, 2014, MOP065.
- [2] E.A. Schneidmiller and M.V. Yurkov, Phys. Rev. ST Accel. Beams 18, 030705 (2015).
- [3] E.A. Schneidmiller and M.V. Yurkov Proc. SPIE 9512, 951219 (May 12, 2015); doi:10.1117/12.2181230.
- [4] N.M. Kroll, P.L. Morton, and M.N. Rosenbluth, IEEE J. Quantum Electron. 17, 1436 (1981).
- [5] T.J. Orzechowski et al., Phys. Rev. Lett. 57, 2172 (1986).
- [6] X.J. Wang, H.P. Freund, D. Harder, W.H. Miner, Jr., J.B. Murphy, H. Qian, Y. Shen, and X. Yang, Phys. Rev. Lett. 103, 154801 (2009).
- [7] P. Emma et al, Nature Photonics 4, 641 (2010).
- [8] Tetsuya Ishikawa et al., Nature Photonics 6, 540 (2012).
- [9] R.A. Jong, E.T. Scharlemann, W.M. Fawley Nucl. Instrum. Methods Phys. Res. A272, 99 (1988)
- [10] W.M. Fawley, Nucl. Instrum. Methods Phys. Res. A375, 550 (1996)
- [11] W.M. Fawley, Z. Huang, K.J. Kim, and N. Vinokurov, Nucl. Instrum. Methods Phys. Res. A483, 537 (2002)
- [12] E.L. Saldin, E.A. Schneidmiller and M.V. Yurkov, Opt. Commun. 95, 141 (1993).
- [13] E.T. Scharlemann, Laser Handbook, Volume 6, Free electron lasers, eds. W.B. Colson, C. Peilegrini and A. Renieri (North Holland, Amsterdam, 1991), p. 291.
- [14] E.L. Saldin, E.A. Schneidmiller and M.V. Yurkov, Physics Reports 260, 187 (1995).
- [15] E.L. Saldin, E.A. Schneidmiller, M.V. Yurkov, "The Physics of Free Electron Lasers" (Springer-Verlag, Berlin, 1999).
- [16] E.L. Saldin, E.A. Schneidmiller, and M.V. Yurkov, Nucl. Instrum. and Methods A 429, 233 (1999).
- [17] P. Krejcik, Talk at IPAC 2014, June 2014, Dresden, Germany.
- [18] Y. Ding, F.-J. Decker, V.A. Dolgashev, J. Frisch, Z. Huang, P. Krejcik, H. Loos, A. Lutman, A. Marinelli, T.J. Maxwell, D. Ratner, J. Turner, J. Wang, M.-H. Wang, J. Welch, and J. Wu, Preprint SLAC-PUB-16105, SLAC National Accelerator Laboratory, 2014.
- [19] W. Ackermann et al., Nature Photonics 1, 336 (2007).
- [20] S. Schreiber and B. Faatz, High Power Laser Science and Engineering e20, 1 (2015). doi:10.1017/hpl.2015.16.
- [21] B. Faatz et al., New journal of physics 18(6), 062002 (2016).
- [22] E.L. Saldin, E.A. Schneidmiller and M.V. Yurkov, Opt. Commun. 281, 1179-1188 (2008).